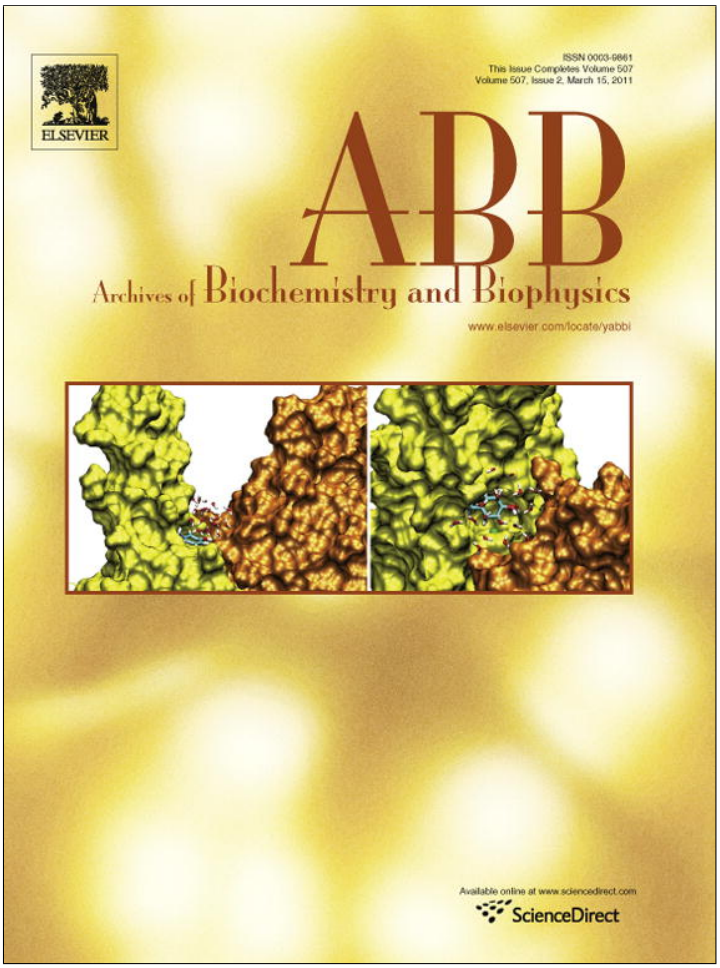

Archives of Biochemistry and Biophysics 507 (2011) 304–309

Contents lists available at ScienceDirect

Archives of Biochemistry and Biophysics

journal homepage: www.elsevier.com/locate/yabbi

Exploring the molecular basis of human manganese superoxide dismutase inactivation mediated by tyrosine 34 nitration

Diego M. Moreno [a], Marcelo A. Martí [b], Pablo M. De Biase [a], Darío A. Estrin [a], Verónica Demicheli [c], Rafael Radi [c], Leonardo Boechi [a,*]

[a] Departamento de Química Inorgánica, Analítica y Química-Física and INQUIMAE-CONICET, Facultad de Ciencias Exactas y Naturales, Universidad de Buenos Aires, Ciudad Universitaria, Pab. 2, C1428EHA Buenos Aires, Argentina
[b] Departamento de Química Biológica and INQUIMAE-CONICET, Facultad de Ciencias Exactas y Naturales, Universidad de Buenos Aires, Ciudad Universitaria, Pab. 2, C1428EHA Buenos Aires, Argentina
[c] Departamento de Bioquímica and Center for Free Radical and Biomedical Research, Facultad de Medicina, Universidad de la República, Av. Gral Flores 2125, CP 11800, Montevideo, Uruguay

ARTICLE INFO

Article history:
Received 5 October 2010
and in revised form 17 November 2010
Available online 15 December 2010

Keywords:
Manganese superoxide dismutase
MnSOD
Tyrosine nitration
Enzyme inactivation
Multiple steered molecular dynamics
MSMD
Free energy
Molecular dynamics
Ligand migration

ABSTRACT

Manganese Superoxide Dismutase (MnSOD) is an essential mitochondrial antioxidant enzyme that protects organisms against oxidative damage, dismutating superoxide radical ($O_2^{\cdot-}$) into H_2O_2 and O_2. The active site of the protein presents a Mn ion in a distorted trigonal–bipyramidal environment, coordinated by H26, H74, H163, D159 and one $^-$OH ion or H_2O molecule. The catalytic cycle of the enzyme is a "ping-pong" mechanism involving Mn^{3+}/Mn^{2+}. It is known that nitration of Y34 is responsible for enzyme inactivation, and that this protein oxidative modification is found in tissues undergoing inflammatory and degenerative processes. However, the molecular basis about MnSOD tyrosine nitration affects the protein catalytic function is mostly unknown.

In this work we strongly suggest, using computer simulation tools, that Y34 nitration affects protein function by restricting ligand access to the active site. In particular, deprotonation of 3-nitrotyrosine increases drastically the energetic barrier for ligand entry due to the absence of the proton.

Our results for the WT and selected mutant proteins confirm that the phenolic moiety of Y34 plays a key role in assisting superoxide migration.

Introduction

Superoxide dismutases (SODs) are enzymes that protect biological systems against oxidative damage caused by superoxide radical ($O_2^{\cdot-}$) which is generated during aerobic metabolism by one electronic reduction process of molecular oxygen through different mechanisms like the catalytic production by flavoproteins like xanthine oxidase [1,2], the mitochondrial respiratory chain [3] or activation of NADPH oxidase [4,5].

There are at least three unrelated families of SODs found in nature: the structurally homologous mononuclear active site iron SODs or manganese SODs (MnSOD)[1], the binuclear copper/zinc SODs and the mononuclear nickel SOD [6–9].

MnSOD is found in mitochondrial matrix and chloroplast of eukaryotes and in the cytoplasm of bacteria. This enzyme was found to be essential in mammals as shown by knockout mice experiments where individuals that did not express MnSOD died within 10 days after birth [10]. Several crystal structures have been published of the wild type (WT) enzyme [11–13] and the active site consists of one Mn ion per unit in a distorted trigonal–bipyramidal environment, coordinated by three histidine residues, one aspartate and one $^-$OH ion or H_2O molecule (Fig. 1) [12,14].

MnSOD is a homotetramer (96 kDa) that has a ring of positive electrostatic charge surrounding the active site, which is suggested to enhance attraction for negatively charged superoxide. Proximal to the catalytic Mn site is the substrate access cavity, which is characterized by a hydrogen-bonded network that is comprised of solvent molecules and several key residues such as Q143, Y34, H30 and Y166, which are needed for proper activity [13,15,16]. Fig. 2 shows the ligand migration pathway to the active site in one monomer in the dimeric structure. Since Y34 is located in the access tunnel, this residue is known to play a central role in the ligand migration process [17].

The proposed MnSOD catalytic cycle consists of a "ping-pong" mechanism which oscillates between metal Mn^{3+}/Mn^{2+} redox states as is schematically depicted in Eqs. (1 and 2) [18,19].

* Corresponding author.
E-mail address: lboechi@qi.fcen.uba.ar (L. Boechi).

[1] *Abbreviations used:* MnSOD, manganese superoxide dismutases; WT, wild type; NY, 3-nitrotyrosine; MSMD, multiple steered molecular dynamics.

0003-9861/$ - see front matter © 2010 Elsevier Inc. All rights reserved.
doi:10.1016/j.abb.2010.12.011

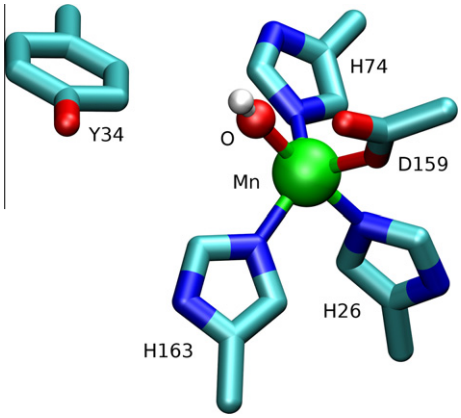

Fig. 1. Active site of MnSOD, showing the Mn center, the three histidines and aspartate residues, the O of the $^{-}OH/H_2O$ and the second sphere residue tyrosine at around 5.6 Å from the metal center.

$$Mn^{3+} + O_2^{\cdot-} \rightarrow Mn^{2+} + O_2 \quad (1)$$

$$Mn^{2+} + O_2^{\cdot-} + 2H^{+} \rightarrow Mn^{3+} + H_2O_2 \quad (2)$$

In the WT enzyme, the high values of the kinetic constants for both half-reactions (1.5 and $1.1 \times 10^9\ M^{-1}s^{-1}$, respectively) [17] might be explained by the presence of a big entry channel which freely leads the superoxide to the active site. Decreasing of kinetic constants could be promoted by the introduction of residues which alter the original tunnel features.

Recent computational studies revealed that the first step, the oxidation of $O_2^{\cdot-}$ to O_2, most likely occurs by an associative mechanism, while the second step seems to take place by a second sphere electron transfer mechanism, i.e., without direct coordination of the second $O_2^{\cdot-}$ substrate to the metal center. These results also interestingly suggest that Y34 plays a key role in the second step catalysis [20,21].

Protein tyrosine nitration is a covalent post-translational protein modification derived from the reaction of proteins with nitrating agents. One of the most relevant nitrating agents *in vivo* is peroxynitrite ($ONOO^-$), a potent oxidant formed by the diffusion-controlled reaction between nitric oxide ($^{\bullet}NO$) and superoxide radical ($O_2^{\cdot-}$) which is involved in a variety of disease states [22–24]. The nitration of protein tyrosines may alter the structure and/or the function of proteins [25–29], although the mechanistic details of the changes for specific proteins at the molecular level are just being unraveled [30].

Human MnSOD is a prime example of a tyrosine nitrated protein with functional consequences *in vivo*. MnSOD contains nine tyrosine residues, one of which (Y34) is highly conserved phylogenetically and is located only a few Å from Mn [13]. The site-specific nitration at this residue that is observed in many inflammatory and degenerative diseases including chronic organ rejection, ischemia/reperfusion, arthritis, atherosclerosis and tumorigenesis [31,32], results in enzyme inactivation [33]. Indeed, *in vitro* studies from several groups indicate that Y34 post- and even co-translationally nitrated human MnSOD is inactive [34–38] and that the Mn atom efficiently directs peroxynitrite and nitric oxide-mediated nitration in the presence of $O_2^{\cdot-}$ to the adjacent Y34 [22,36,37] which is at only 5 Å from the metal center. The detoxification function of MnSOD is essential to normal cell and mitochondrial homeostasis and therefore significant decreases in its activity as observed during tyrosine nitration results in mitochondrial oxidative stress with potential consequences in bioenergetics and signaling of cell death [32,39].

Understanding how MnSOD Y34 nitration (or replacement) alters MnSOD function at the molecular level is not an easy task. The replacement of Y34 by other amino acids results in a large reduction in catalysis efficiency [17,34,40,41], confirming a key role of this conserved amino acid in the dismutation reaction mechanism. For example, *in vitro* enzyme kinetics studies obtained Y34F mutant, yielded values of k_{cat}/K_M that are similar to those of the WT ($\approx 800\ \mu M^{-1}s^{-1}$), but there is a decrease of ten fold in the k_{cat} value, [42] suggesting the crucial role of Y34 hydroxyl group in both substrate binding and catalysis. Also, replacement of Y34 ortho hydrogen by a fluorine atom (3-fluorotyrosine) [41] which represents a minor steric change reduces the catalytic activity k_{cat}/K_M to $30\ \mu M^{-1}s^{-1}$. Finally, it should be noted that the actual observed k_{cat}/K_M value of $\approx 800\ \mu M^{-1}s^{-1}$ for the WT enzyme, is close to that expected for a diffusion-controlled reaction, strongly suggesting that superoxide access to the Mn active site is the rate limiting step [43]. This point confirms the idea that an obstruction or a charge density modification in the channel access could be the reason for the lack of activity in modified MnSOD enzymes.

Based on these results, several hypotheses have been put forward to explain the effect of Y34 nitration. The crystal structure of nitrated human MnSOD has been published [16] and shows that replacement of Y34 by 3-nitrotyrosine (NY) does not cause significant conformational changes of active-site residues or solvent displacement. This modification, however, has other effects; for example in a change in the pKa of the tyrosine phenol group, from around 10 to 7.5 [22,34,44], which may interrupt the hydrogen bonding network of the Y34-Q143 pair, affecting the catalytic

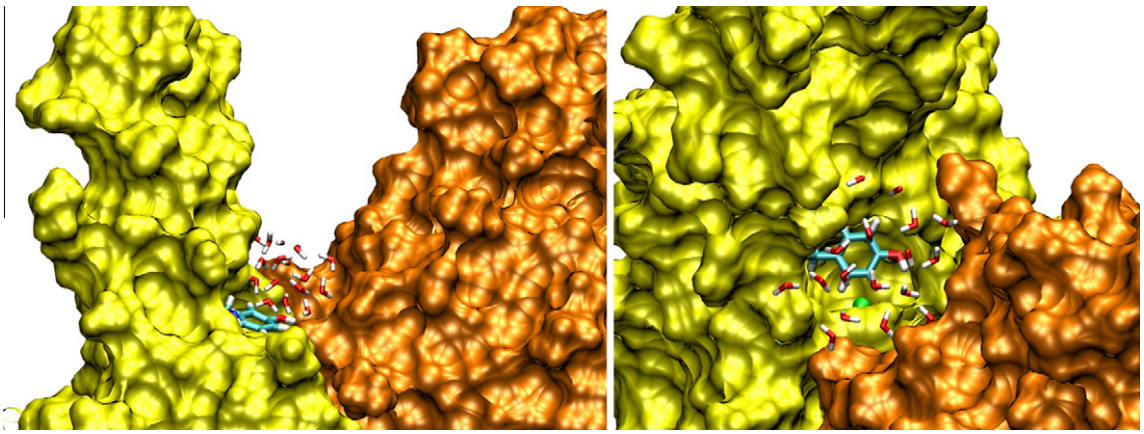

Fig. 2. Two different view (left and right panel) of surface contour analysis of the dimeric WT-MnSOD (each subunit depicted in different colors, Mn coordinated residues were excluded of the analysis). Manganese atom (green), Y34 (cyan), and several water molecules (red/white) are depicted in order to shed light on the accessibility to the active site. (For interpretation of the references to colour in this figure legend, the reader is referred to the web version of this article.)

cycle. Another possibility arises from the fact that NY34 is located at the end of the access channel and the nitro group is expected to show steric as well as electrostatic effects that impact the access and/or binding of superoxide substrate into the active site.

In order to contribute to the elucidation of the molecular basis of MnSOD inactivation by tyrosine nitration, we focused our attention on how modifications of Y34 modulate the entry of the superoxide substrate from the solvent into the active site. We performed Multiple Steered Molecular Dynamics (MSMD) simulations, to compute the free energy profiles of superoxide migration in the WT and in several modified proteins: Y34F, Y34V, and the nitrated NY34 in both protonated and deprotonated states. Our results show that the presence of the nitro group in NY34 completely blocks the superoxide ligand migration entry path, inactivating the enzyme. An important role of the polar hydrogen of Y34 is also proposed.

Methods

Molecular dynamics simulations

All simulations were performed starting from the crystal structure of Human Manganese Superoxide Dismutase (MnSOD), determined at 2.20 Å resolution [Protein Data Bank (PDB) entry 1ABM] [13]. Each simulation was performed using monomeric WT protein, or single mutant proteins (Y34F, Y34V, Y34NY) built *in silico*. The systems were then immersed in a box of TIP3P water molecules [45]. The minimum distance between the protein and wall was 12 Å. All systems were simulated employing periodic boundary conditions and Ewald sums for treating long-range electrostatic interactions [46]. The shake algorithm was used to keep bonds involving the H atom at their equilibrium length. This allowed us to employ a 2 fs time step for the integration of Newton's equations. The parm99 and TIP3P force fields implemented in AMBER [47] were used to describe the protein and water, respectively [48]. The temperature and pressure were regulated with the Berendsen thermostat and barostat, respectively, as implemented in AMBER [47]. The cut off used was 10 Å for the van der Waals interactions. All systems were firstly minimized to optimize any possible structural clashes. Subsequently, the systems were heated slowly from 0 to 300 K using a time step of 0.1 fs, under constant volume conditions. Finally, a short simulation at a constant temperature of 300 K under a constant pressure of 1 bar was performed using a time step of 0.1 fs, to allow the systems to reach proper density. These equilibrated structures were the starting point for 10 ns of MD simulations.

The parameters for active site atoms (Mn, $^{-}$OH, Asp and His) were taken from literature [49]. The charges and parameters of nitrated tyrosine and free superoxide radical were determined using ab initio methods. The van der Waals radius, force constants and equilibrium distances, angles and dihedral for the nitro group in nitrotyrosine were taken from gaff database [47]. For the tyrosine group in nitro-tyrosine we used parm99 parameters. Partial charges were RESP charges computed using Hartree–Fock method and 6-31G* basis set [50] (see Table 1 in Supplementary Material).

Calculation of substrate entry free energy profiles

In order to examine the accessibility of the active site in the different structures of MnSOD, free energy profiles of superoxide migration were determined for each system. The profiles were computed by means of constant velocity multiple steered molecular dynamics (MSMD) simulations, and using the Jarzynski's equality [51], a method which has been successfully applied for ligand migration studies in several works from our group [52–55]. Briefly, in the MSMD method the ligand is slightly pulled in the active site, using a time dependent harmonic restraint potential. In the present case the chosen reaction coordinate ξ was, the $Mn–O_{superoxide}$ distance. The harmonic potential force constant used was 200 kcal mol^{-1} Å^{-2}. The pulling velocities used were 25 Å/ns. To construct the free energy profile of ligand migration along a selected tunnel, a set of 30 independent MSMD simulations were performed, each one starting from an equilibrated MD structure (or snapshot), where the superoxide ligand is outside the protein at 10 Å distance of the Mn. In order to check starting structures cover a wide range of MnSOD entry locations, we scan different entry angles along the equilibrium MD simulation (from which the starting MSMD snapshots are taken). The position of the superoxide substrate covers a wide range of possible entrance pathways (see Fig. S1 in Supplementary Material). Convergence of each profile was determined by computing the exponential averages, using an increasing number of individual work profiles, until no significant change in the resulting profile were obtained with the incorporation of new work profiles. This is shown in Figs. S2–6 of Supplementary Materials, where free energy profiles computed using 10, 15, 20, 25, and 30 individual MSMD simulations are depicted. As can be seen after 20 to 30 MSMD simulations the resulting free energy profile does not change significantly due to the addition of new simulations. This computational scheme has been successfully applied to compute the free energy profile of ligand migration in heme proteins and also to compute free energy profiles of enzymatic reactions [52–54].

Results and discussion

Free energy profile of WT MnSOD

We computed the free energy profile for superoxide access to active site Mn in WT MnSOD. The resulting profile presented in Fig. 3, shows that there is no barrier for ligand entrance until the superoxide is 7–8 Å from the Mn. In fact, a slight dip in the energy profile is found at what appears to be a small secondary docking site (Site 1).

This result is in agreement with other theoretical and experimental investigations which observed a second-sphere binding site at 5–7.5 Å from the metal center, in the vicinity of Y34 and H30 residues [49,56]. A visual inspection of the corresponding snapshots along the simulation shows that in Site 1 the superoxide substrate interacts with H30 and/or H163 as shown in Fig. 4.

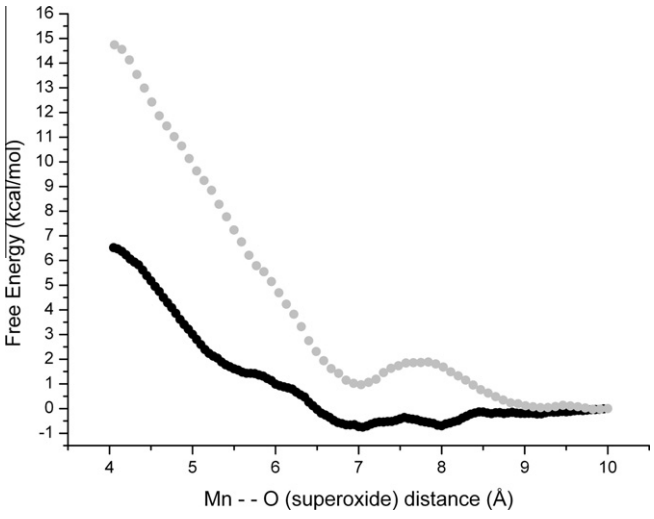

Fig. 3. Free energy profile for O_2^- migration along the diffusion pathway using the distance from the Mn atom to one of the O in O_2^- as the driven coordinate. WT and Y34NY proteins are depicted using solid line and grey dots, respectively.

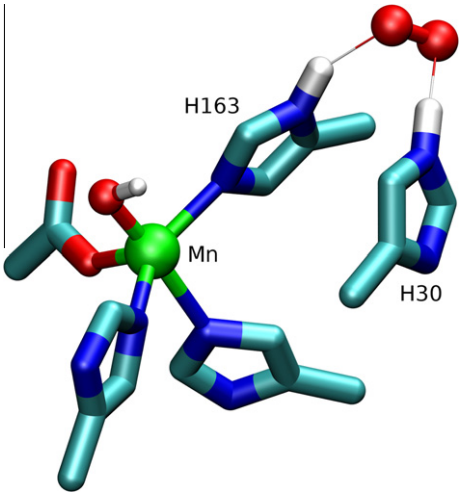

Fig. 4. Representation of the second binding site at about 7 Å of the metal center in the vicinity of H30. Superoxide interactions by hydrogen bonds with H30 and/or H163 are depicted with fine straight lines.

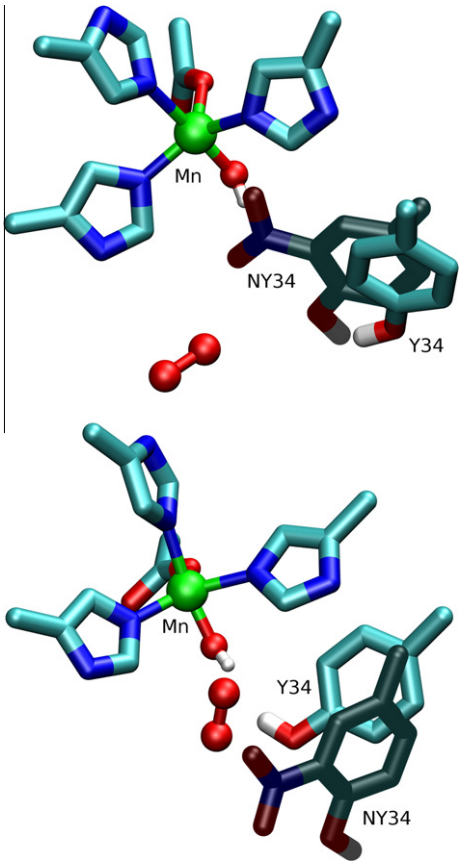

Fig. 5. A representative snapshot of the MSMD simulation, showing WT and Y34NY actives sites, in which the nitro group is blocking substrate access (top panel). The last position adopted by the ligand during the free energy profile simulations (low panel).

After leaving Site 1 superoxide is stabilized by a hydrogen bond (HB) to Y34 which facilitates the entry to the active site (Fig. 5). The breaking of 1 to 2 HB from Site 1, while establishing one HB with Y34, results in the 2 kcal/mol free energy increase from 7 to 5 Å. At this point the HB between Y34 and the superoxide begins to break resulting in a sharp increase in free energy, until reaching the Mn active site. The overall superoxide entry barrier for the WT enzyme is around 6 kcal/mol.

Free energy profile of nitrated MnSOD

We now analyze the effect of Y34 nitration on the resulting profile which is presented together with that for WT MnSOD in Fig. 3. Preliminary MD results showed that the orientation of the nitro group did not change during the time scale of the simulations. It points toward the metal center in the vicinity of the superoxide channel of entrance. On the other hand, the hydroxyl group can flip towards or away from the nitro group.

The free energy profile for superoxide migration in nitrated MnSOD presented a small 2 kcal/mol barrier in the vicinity of Site 1. This barrier is possibly related to the electrostatic repulsion of the nitro group that slightly repels the substrate out of the channel entrance. After crossing this small barrier the H-bond with H30 and H163 stabilizes superoxide in Site 1 (at 7 Å) as it was observed previously in the WT enzyme.

In the vicinity of the Mn atom (between 4 and 7 Å) the free energy profile presents a barrier of about 15 kcal/mol (about 8 kcal/mol larger than that for the WT enzyme). A microscopical analysis strongly suggests that the significant increase in the barrier is due to both steric and electrostatic effects of the nitro group, which blocks the active site (Fig. 5). Contrary to what is observed for the WT protein, the superoxide needs to displace the nitrotyrosine with the associated energy cost to bind to Mn. The displacement is also evident from Fig. 6 where we observe that the hydroxyl group of the 3-nitrotyrosine is close to the metal center until the superoxide reaches a Mn distance of 5 Å, where the nitrotyrosine suddenly moves away from the active site to allow superoxide access. Furthermore, nitration and displacement, also results in the Y34 phenol group pointing away from the active site (contrary to what is observed for the WT enzyme), as shown in Fig. 5, forbidding therefore any involvement of this group in the catalytic reaction.

Since a very important change that nitrated tyrosines undergo is the change in pKa of the phenol group, we evaluated the accessibility of superoxide to the active site in the nitrated and deprotonated tyrosine 34 case (deprotonated NY34). An important consideration is that the pKa of the phenol group in nitrotyrosine in proteins may be significantly different to that of free nitrotyrosine depending on the polarity of the environment; indeed, the pKa

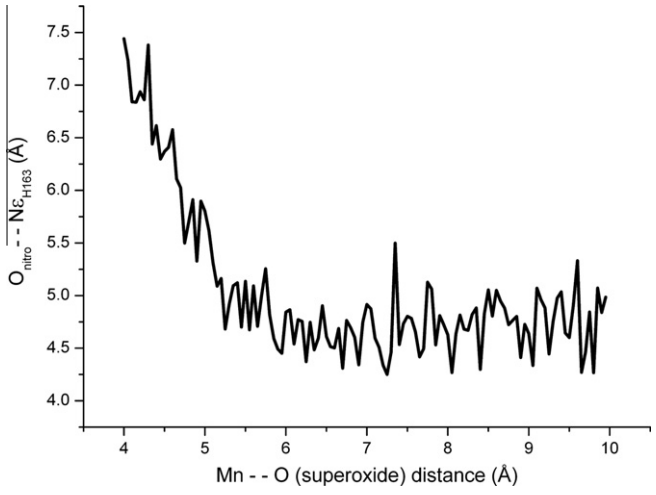

Fig. 6. Representation of the displacement of NY34 during a MSMD simulation plotting the distance between one of the oxygen atom of the nitro group in NY34 and the Nε of H163 vs. the distance of superoxide from the metal center.

of nitrotyrosine can substantially increase towards the alkaline range in polar protein microenvironments [44]. In the case of MnSOD, even though there is no a direct experimental report for the pKa of NY34, we can safely estimate that its pKa would be very similar to that of free nitrotyrosine (e.g. 7.4–7.8) because of its solvent accessibility. Therefore, one can expect that under physiological pH (ca. 7.4) a large proportion of the phenol group (40–50%) would be in its dissociated form as phenolate. Thus, we calculated the free energy profile for deprotonated NY34 in order to compare the effect of the protonation state on ligand accesibility. Comparison of the two profiles (protonated and deprotonated NY34) presents a few particularly interesting points to be detailed. Accessibility from the solvent to the docking Site 1 is not affected by deprotonation of NY34, as both profiles are nearly identical from 10 to 7 Å (Fig. S7). Nevertheless, when superoxide is passing near deprotonated NY34 (from 7 to 4 Å) a barrier of about 30 kcal/mol appears (about 15 kcal/mol larger than that of the protonated NY34 case, and about 23 kcal/mol larger than that of the WT enzyme). This finding is consistent as there are multiple effects to consider: the electrostatic repulsion between the superoxide and both the negatively charged nitro group and the phenolate moiety.

These results clearly indicate that nitration of Y34 blocks the accessibility of superoxide, inactivating MnSOD. Moreover we have shown that polar hydrogen of the tyrosine sidechain is critical for the overall function of the protein.

Free energy profiles of Y34 mutant proteins

To further analyze the role of Y34 and understand how tyrosine nitration significantly increases the barrier for superoxide access to the active site, we computed now the corresponding profile for Y34F and Y34V mutants. The obtained energy profiles are shown in Fig. 7.

The barriers to reach the Mn are around 11 kcal/mol in Y34F (4 kcal/mol higher compare to WT case) and 8 kcal/mol in Y34V (slightly higher compared to the WT case). The higher barrier of the Y34F protein, clearly shows that the Y34 phenol group stabilizes the superoxide close to the Mn, thereby lowering the overall barrier. The polar environment effect is further confirmed by the Y34V mutant, which although smaller is also hydrophobic. When Y34V is compared with Y34F MnSOD a 5 kcal/mol difference in the barrier is observed, evidencing the presence of steric effects. Indeed, analysis of the structures of both proteins when superoxide

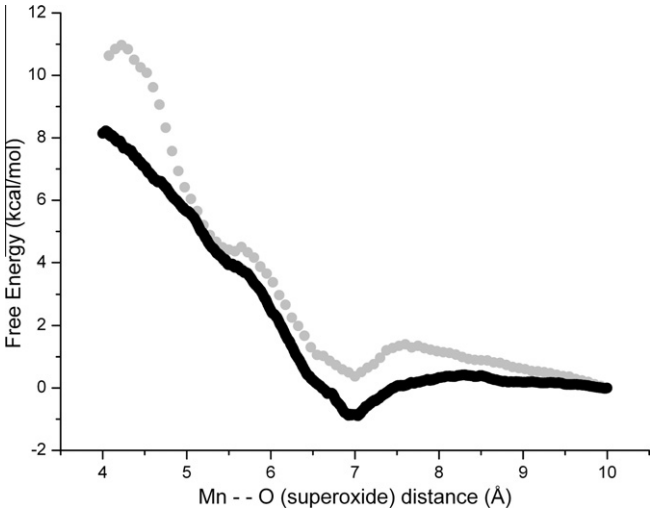

Fig. 7. Free energy profile for O_2^- migration along the diffusion pathway in Y34F (dot) and Y34V (solid line); the distance from the Mn atom to one of the O in O_2^- is used as the driven coordinate.

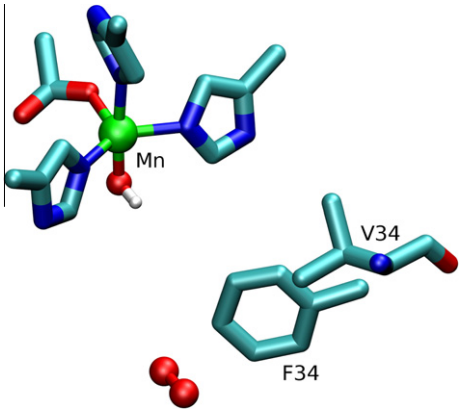

Fig. 8. A snapshot from Y34F and Y34V proteins, in which the difference in the sterical effect causes by the aromatic ring of F34 is ilustrated.

is around 4–5 Å from the Mn, (Fig. 8) clearly shows that the volume of F34 aromatic rings produces higher steric effects compared to the methyl groups of Val-34. Nevertheless, Y34V also displays a slightly higher barrier compared to WT protein, since the higher accessibility is compensated by the lack of Y–OH superoxide stabilizing interactions.

General implications for tyrosine nitrated proteins

Knowing the functional outcome of a nitrated protein (*i.e.* loss, none or gain of function) is a key issue for determining whether the presence of a given nitrated protein is cause or consequence in the pathogenesis of a variety of disease conditions. The results presented herein provide an explanation at the molecular level on how Y34 nitration in human MnSOD leads to enzyme inactivation; in addition, the data underscore the relevance of performing similar mechanistic studies to understand the effect of tyrosine nitration in other proteins. The use of computation methodologies appears as an interesting and appealing alternative technique to experimental measurements specially when obtaining high yields of nitrated proteins at specific positions *in vitro,* and/or revealing mechanistic aspects at the atomic level, turn to be difficult.

Conclusions

We have performed a detailed study of superoxide entrance to wild type, nitrated and mutant (Y34F and Y34V) human MnSOD using MSMD simulations, in order to determine the molecular basis of its inactivation by nitration. Our results show that the introduction of the bulky negatively polarized substituent in Y34 produces an electrostatic and steric repulsion which is reflected in a dramatic increase of the free energy profile for superoxide access to the metal center, resulting in a blocked channel and inactive enzyme. This barrier is even higher when taking into account the deprotonated NY34 species, which becomes relevant in the presence of the nitro group. Therefore, the overall barrier of NY34 MnSOD results in a blocked channel and an inactive enzyme. These results, supported by the Y34F and Y34V results, provide strong evidence for the role of both nitration of Y34 as one possible way to inactivate the protein, and the phenol group of Y34 controlling the correct function of MnSOD.

Acknowledgments

This work was partially supported by grants from Universidad de Buenos Aires X625 to MAM and X074 to DAE, ANPCYT 07-1650 to MAM and 06-25667 to DAE, CONICET PIP 01207 and

Guggenheim Foundation grant awarded to DAE. We acknowledge the financial support to the EU FP7 program (projects Nostress). DAE and MAM are members of CONICET. DMM, LB and PMD thank CONICET for postdoctoral and PhD fellowships. RR was supported by a grant of the Howard Hughes Medical Institute. VD was partially supported by a PhD fellowship from Agencia Nacional de Investigación e Innovación (ANII, Uruguay). Computer power was provided by the Centro de computación de alto rendimiento (C.E.C.A.R.) at the FCEN-UBA and by the cluster MCG PME N° 2006-01581 at the Universidad Nacional de Cordoba. RR is a Howard Hughes International Research Scholar.

Appendix A. Supplementary data

Supplementary data associated with this article can be found, in the online version, at doi:10.1016/j.abb.2010.12.011.

References

[1] J.M. McCord, I. Fridovich, J. Biol. Chem. 243 (1968) 5753–5760.
[2] P.F. Knowles, J.F. Gibson, F.M. Pick, R.C. Bray, Biochem. J. 111 (1969) 53–58.
[3] A. Boveris, E. Cadenas, FEBS Lett. 54 (1975) 311–314.
[4] Y. Suzuki, R.I. Lehrer, J. Clin. Invest. 66 (1980) 1409–1418.
[5] B.M. Babior, Am. J. Med. 109 (2000) 33–44.
[6] B. Halliwell, J.M.C. Gutteridge, Free Radical Biology and Medicine, Clarendon Press, Oxford, 1999.
[7] I. Pálinkó, J.G. Huges, A.J. Robinson, in: Frank H. Columbus (Ed.), Inorganic Biochemistry: Research Progress, Nova Science Publishers Inc., New York, 2008, pp. 281–303.
[8] I. Fridovich, Annu. Rev. Biochem. 64 (1995) 97–112.
[9] A. Merlino, I.R. Krauss, I. Castellano, E.D. Vendittis, B. Rossi, M. Conte, A. Vergara, F. Sica, J. Struct. Biol. 172 (2010) 343–352.
[10] Y. Li, T.-T. Huang, E.J. Carlson, S. Melov, P.C. Ursell, J.L. Olson, L.J. Noble, M.P. Yoshimura, C. Berger, P.H. Chan, D.C. Wallace, C.J. Epstein, Nat. Genet. 11 (1995) 376–381.
[11] M.L. Ludwig, A.L. Metzger, K.A. Pattridge, W.C. Stallings, J. Mol. Biol. 219 (1991) 335–358.
[12] R.A. Edwards, H.M. Baker, M.M. Whittaker, J.W. Whittaker, G.B. Jameson, E.N. Baker, J. Biol. Inorg. Chem. 3 (1998) 161.
[13] G.E.O. Borgstahl, H.E. Parge, M.J. Hickey, W.F. Beyer, R.A. Hallewell, J.A. Tainer, Cell 71 (1992) 107–118.
[14] L. Noodleman, T. Lovell, W.G. Han, J. Li, F. Himo, Chem. Rev. 104 (2004) 459.
[15] I. Ayala, J.J.P. Perry, J. Szczepanski, J.A. Tainer, M.T. Vala, H.S. Nick, D.N. Silverman, Biophys. J. 89 (2005) 4171–4179.
[16] P. Quint, R. Reutzel, R. Mikulski, R. McKenna, D.N. Silverman, Free Rad. Biol. Med. 40 (2006) 453–458.
[17] J.J.P. Perry, A.S. Hearn, D.E. Cabelli, H.S. Nick, J.A. Tainer, D.N. Silverman, Biochemistry 48 (2009) 3417–3424.
[18] C. Bull, E.C. Niederhoffer, T. Yoshida, J.A. Fee, J. Am. Chem. Soc. 113 (1991) 4069–4076.
[19] J.-L. Hsu, Y. Hsieh, C. Tu, D. O'Connor, H.S. Nick, D.N. Silverman, J. Biol. Chem. 271 (1996) 17687–17691.
[20] L. Rulísek, K.P. Jensen, K. Lundgren, U. Ryde, J. Comput. Chem. 27 (2006) 1398–1414.
[21] M. Srnec, F. Aquilante, U. Ryde, L. Rulísek, J. Phys. Chem. B 113 (2009) 6074–6086.
[22] R. Radi, Natl. Acad. Sci. USA 101 (2004) 4003–4008.
[23] H. Ischiropoulos, Arch. Biochem. Biophys. 356 (1998) 1–11.
[24] G. Ferrer-Sueta, R. Radi, ACS Chem. Biol. 4 (2009) 161–177.
[25] M.D. Gole, J.M. Souza, I. Choi, C. Hertkorn, S. Malcolm, R.F. Foust III, B. Finkel, P.N. Lanken, H. Ischiropoulos, J. Physiol. Lung Cell Mol. Physiol. 278 (2000) L961–967.
[26] A.M. Cassina, R. Hodara, J.M. Souza, L. Thomson, L. Castro, H. Ischiropoulos, B.A. Freeman, R. Radi, J. Biol. Chem. 275 (2000) 21409–21415.
[27] O. Guittet, B.a. Ducastel, J.S. Salem, Y. Henry, H. Rubin, G.v. Lemaire, M. Lepoivre, J. Biol. Chem. 273 (1998) 22136–22144.
[28] C. Batthyány, J.M. Souza, R. Durán, A. Cassina, C. Cerveñansky, R. Radi, Biochemistry 44 (2005) 8038–8046.
[29] M. Zou, C. Martin, V. Ullrich, Biol. Chem. 378 (1997) 707–713.
[30] L.A. Abriata, A. Cassina, V. Tórtora, M. Marín, J.M. Souza, L. Castro, A.J. Vila, R. Radi, J. Biol. Chem. 284 (2009) 17–26.
[31] D.L. Cruthirds, L. Novak, K.M. Akhi, P.W. Sanders, J.A. Thompson, L.A. MacMillan-Crow, Arch. Biochem. Biophys. 412 (2003) 27–33.
[32] L.A. Macmillan-Crow, D.L. Cruthirds, Free Radic. Res. 34 (2001) 325–336.
[33] L.A. MacMillan-Crow, J.P. Crow, J.D. Kerby, J.S. Beckman, Proc. Natl Acad. Sci. USA 93 (1996) 11853–11858.
[34] F. Yamakura, H. Taka, T. Fujimura, K. Murayama, J. Biol. Chem. 273 (1998) 14085–14089.
[35] L.A. MacMillan-Crow, J.P. Crow, J.A. Thompson, Biochemistry 37 (1998) 1613–1622.
[36] C. Quijano, D. Hernandez-Saavedra, L. Castro, J.M. McCord, B.A. Freeman, R. Radi, J. Biol. Chem. 276 (2001) 11631–11638.
[37] V. Demicheli, C. Quijano, B. Alvarez, R. Radi, Free Rad. Biol. Med. 42 (2007) 1359–1368.
[38] H. Neumann, J.L. Hazen, J. Weinstein, R.A. Mehl, J.W. Chin, J. Am. Chem. Soc. 130 (2008) 4028–4033.
[39] R. Radi, A. Cassina, R. Hodara, C. Quijano, L. Castro, Free Radical Biol. Med. 33 (2002) 1451–1464.
[40] H. Ischiropoulos, L. Zhu, J. Chen, M. Tsai, J.C. Martin, C.D. Smith, J.S. Beckman, Arch. Biochem. Biophys. 298 (1992) 431–437.
[41] X. Ren, C. Tu, D. Bhatt, J.J.P. Perry, J.A. Tainer, D.E. Cabelli, D.N. Silverman, J. Mol. Struct. 790 (2006) 168–173.
[42] Y. Guan, M.J. Hickey, G.E.O. Borgstahl, R.A. Hallewell, J.R. Lepock, D. O'Connor, Y.S. Hsieh, H.S. Nick, D.N. Silverman, J.A. Tainer, Biochemistry 37 (1998) 4722.
[43] W.H. Bannister, J.V. Bannister, Free Radical Res. Commun. 4 (1987) 1–13.
[44] K. Yokoyama, U. Uhlin, J. Stubbe, J. Am. Chem. Soc. 132 (2010) 8385–8397.
[45] W.L. Jorgensen, J. Chandrasekhar, J.D. Madura, R.W. Impey, M.L. Klein, J. Chem. Phys. 79 (1983) 926.
[46] B.A. Luty, I.G. Tironi, Chem. Phys. 103 (1995) 3014.
[47] D.A. Case, T. A. Darden, T. E.Cheatham, C. L. Simmerling, J. Wang, R.E. Duke, R. Luo, M. Crowley, R.C. Walker, W. Zhang, K. M. Merz, B. Wang, S. Hayik, A. Roitberg, G. Seabra, I. Kolossvry, K.F. Wong, F. Paesani, J. Vanicek, X. Wu, S. R. Brozell, T. Steinbrecher, H. Gohlke, L. Yang, C. Tan, J. Mongan, V. Hornak, G. Cui, D.H. Mathews, M.G. Seetin, C. Sagui, V. Babin, P.A. Kollman, Amber 10, University of California: San Francisco, 2008.
[48] D.A. Pearlman, D.A. Case, J.W. Caldwell, W.S. Ross, T.E. Cheatham, S. DeBolt, D. Ferguson, G. Seibel, P. Kollman, Comp. Phys. Commun. 91 (1995) 1–41.
[49] L. Rulisek, U. Ryde, J. Phys. Chem. B 110 (2006) 11511–11518.
[50] C.I. Bayly, P. Cieplak, W. Cornell, P.A. Kollman, J. Phys. Chem. 97 (1993) 10269–10280.
[51] C. Jarzynski, Phys. Rev. Lett. 78 (1997) 2690–2693.
[52] A. Bidon-Chanal, M.A. Martí, A. Crespo, M. Milani, M. Orozco, M. Bolognesi, F.J. Luque, D.A. Estrin, Proteins 64 (2006) 457–464.
[53] L. Boechi, M.A. Martí, M. Milani, M. Bolognesi, F.J. Luque, D.A. Estrin, Proteins 73 (2008) 372–379.
[54] L. Boechi, P. Arroyo Mañez, F.J. Luque, M.A. Marti, D.A. Estrin, Proteins 78 (2010) 962–970.
[55] P.M. De Biase, D. Alvarez Paggi, F. Doctorovich, P. Hildebrandt, D.A. Estrin, D.H. Murgida, M.A. Marti, J. Am. Chem. Soc. 131 (2009) 16248–16256.
[56] A.F. Miller, Handbook of Metalloproteins, John Wiley & Sons Inc., 2001.